

# Redox-Noninnocent Behavior of Tris(2-pyridylmethyl)amine Bound to a Lewis Acidic Rh(III) Ion Induced by C–H Deprotonation

Hiroaki Kotani,<sup>†</sup> Takumi Sugiyama,<sup>†</sup> Tomoya Ishizuka,<sup>†</sup> Yoshihito Shiota,<sup>‡</sup> Kazunari Yoshizawa,<sup>‡,§</sup> and Takahiko Kojima<sup>\*,†</sup>

<sup>†</sup>Department of Chemistry, Graduate School of Pure and Applied Sciences, University of Tsukuba, 1-1-1 Tennoudai, Tsukuba, Ibaraki 305-8571, Japan

<sup>‡</sup>Institute for Materials Chemistry and Engineering, Kyushu University, Motooka, Nishi-Ku, Fukuoka 819-0395, Japan

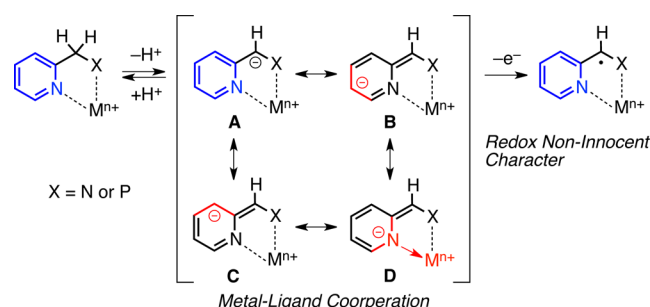
<sup>§</sup>Elements Strategy Initiative for Catalysts & Batteries, Kyoto University, Nishikyo-ku, Kyoto 615-8520, Japan

## Supporting Information

**ABSTRACT:** Rh(III) complexes having tris(2-pyridylmethyl)amine (TPA) and its derivative as tetradentate ligands showed reversible deprotonation at a methylene moiety of the TPA ligands upon addition of a strong base as confirmed by spectroscopic measurements and X-ray crystallography. Deprotonation selectively occurred at the axial methylene moiety rather than equatorial counterparts because of the thermodynamic stability of corresponding deprotonated complexes. One-electron oxidation of the deprotonated Rh(III)–TPA complex afforded a unique TPA radical bound to the Rh(III) center by a ligand-centered oxidation. This is the first example to demonstrate emergence of the redox-noninnocent character of the TPA ligand.

Metal–ligand cooperation has been recognized as one of new methods to develop novel and striking functionality of metal complexes and often derives from pyridine-based ligands.<sup>1</sup> Milstein et al. have reported that a novel Ru catalyst having a pyridine-based PNN pincer ligand is capable of driving the C–H bond activation of alcohols and amines, triggered by deprotonation and synergetic dearomatization processes of the ligand by the metal–ligand cooperation.<sup>2</sup> The deprotonated complex is produced as a key intermediate and stabilized by the contribution of a dearomatized resonance structure among plausible resonance structures (Scheme 1),<sup>3</sup> although the free pyridylmethyl group is not acidic without metal coordination. In fact, the contribution of dearomatized resonance structures was

Scheme 1



suggested by crystal structures of deprotonated complexes in light of bond lengths in the ligand.<sup>3</sup>

In contrast, ligand deprotonation has been known to induce redox-noninnocent character in an originally redox-innocent ligand.<sup>4</sup> For instance, Grützmacher et al. have reported successful isolation of a Rh(I) complex with an aminyl radical by one-electron oxidation of a deprotonated Rh(I)–amido complex.<sup>5</sup> Also, de Bruin et al. have reported ligand oxidation of a deprotonated Ir(I)–BPA complex (BPA = bis(2-picoly)amine) to form a radical ligand.<sup>6</sup> However, these sequential deprotonation and oxidation processes of deprotonated ligands have been limited to the case of metal complexes having NH groups in the ligand as deprotonation sites. To expand the scope of applicable ligands without NH groups as the deprotonation site, a combination of metal–ligand cooperation and subsequent ligand oxidation is required because a variety of radical intermediate-bound metal complexes ( $[M^{n+}(L^{\bullet})]^{n+}$ ) have been investigated as models of galactose oxidase to realize the importance of the radical character of the ligand.<sup>7</sup>

The concept of metal–ligand cooperation is expected to be expanded to metal complexes having versatile and well-known chelating ligands without NH groups. In contrast to the aforementioned BPA ligand, tripodal pyridylamine ligands such as tris(2-pyridylmethyl)amine (TPA) have no easily removable protons, and only methylene protons can be deprotonated.<sup>8,9</sup> So far, a large number of investigations of metal–TPA complexes have been reported with regard to their reactivity in oxidation reactions and in O<sub>2</sub> activation chemistry.<sup>10</sup> However, there is no report on the observation of a metal complex having deprotonated TPA as a ligand and redox-noninnocent behavior of any metal-bound TPA derivatives.

We report herein unique deprotonation from the TPA ligand bound to a Lewis acidic Rh(III) center via metal–ligand cooperation (Scheme 1), and subsequent one-electron oxidation of a deprotonated complex allows us to investigate redox-noninnocent behavior of the TPA ligand. The Rh(III) ion was selected to stabilize the deprotonated species<sup>11</sup> toward further chemical manipulation on the basis of its Lewis acidity and to perform oxidation of the deprotonated ligand based on the redox-inactive character, which fixes the oxidation state to be the

Received: June 16, 2015

Published: August 24, 2015

Rh(III) state as a result of the instability of the Rh(II) and Rh(IV) states in the TPA environment.<sup>10c</sup>

Synthesis of  $[\text{Rh}^{\text{III}}(\text{Cl})_2(\text{L}_1\text{-H6})](\text{Cl})$ <sup>12a</sup> and  $[\text{Rh}^{\text{III}}(\text{Cl})_2(\text{L}_2\text{-H6})](\text{PF}_6)$  ( $\text{L}_2\text{-H6}$ : TPACOOMe = tris(5-methoxycarbonyl-2-pyridylmethyl)amine<sup>12b</sup>) was accomplished by synthesis routes described in the [Supporting Information](#). The methoxycarbonyl (COOMe) groups were introduced to the 5-positions of all pyridine rings to stabilize the deprotonated complex (*vide infra*). The crystal structure of  $[\text{Rh}^{\text{III}}(\text{Cl})_2(\text{L}_2\text{-H6})](\text{PF}_6)$  was determined by X-ray crystallography ([Figure 1c](#)). Note that the impact

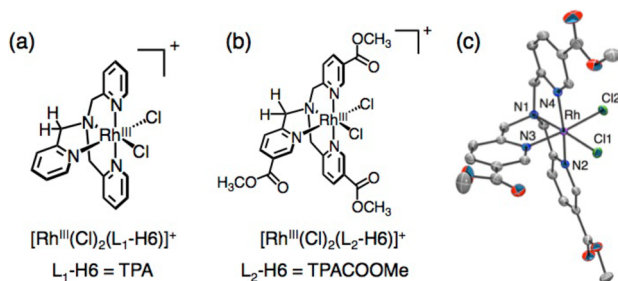


**Figure 1.** (a and b) Chemical structures of Rh(III) complexes used in this study. (c) An ORTEP drawing of  $[\text{Rh}^{\text{III}}(\text{Cl})_2(\text{L}_2\text{-H6})]^+$ .

of introduction of the COOMe groups on the structural parameters of  $[\text{Rh}^{\text{III}}(\text{Cl})_2(\text{L}_2\text{-H6})]^+$  is negligible; there is no difference ( $<0.01$  Å) in the Rh–N<sub>x</sub> ( $x = 1\text{--}4$ ) bond lengths between  $[\text{Rh}^{\text{III}}(\text{Cl})_2(\text{L}_1\text{-H6})]^+$  and  $[\text{Rh}^{\text{III}}(\text{Cl})_2(\text{L}_2\text{-H6})]^+$  ([Table S2](#)). Upon addition of a strong base such as potassium *tert*-butoxide (KO<sup>t</sup>Bu) or KOH into a DMSO-*d*<sub>6</sub> solution containing  $[\text{Rh}^{\text{III}}(\text{Cl})_2(\text{L}_1\text{-H6})]^+$ , a drastic change of the <sup>1</sup>H NMR spectrum was observed ([Figure 2](#)).<sup>13</sup> The <sup>1</sup>H NMR signals of deprotonated

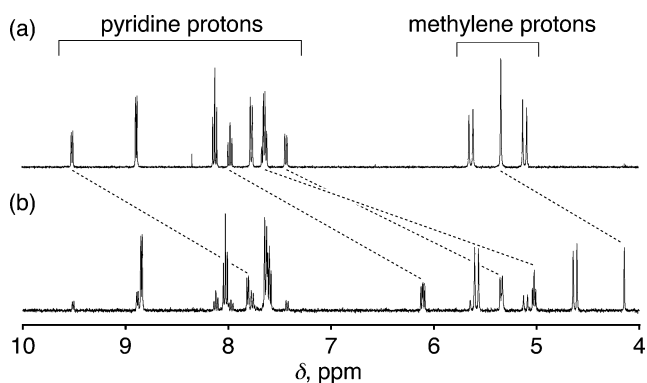


**Figure 2.** <sup>1</sup>H NMR spectra of (a)  $[\text{Rh}^{\text{III}}(\text{Cl})_2(\text{L}_1\text{-H6})]^+$  (2.1 mM) and (b)  $[\text{Rh}^{\text{III}}(\text{L}_1\text{-H5})(\text{Cl})_2]$  obtained upon addition of KOH (5.0 mM) in DMSO-*d*<sub>6</sub> at 298 K under Ar. Dotted lines denote the chemical shift of the axial pyridine moiety before and after deprotonation process.

complexes were assigned by <sup>1</sup>H–<sup>1</sup>H COSY spectroscopy ([Figure S1](#)). The <sup>1</sup>H NMR signals due to the axial pyridine moiety of  $[\text{Rh}^{\text{III}}(\text{L}_1\text{-H5})(\text{Cl})_2]$  ( $\text{L}_1\text{-H5}$ : deprotonated TPA) were revealed to show a larger change of chemical shifts in comparison with those assigned to the equatorial pyridine moieties by the deprotonation. Also, peak integration of the singlet signal at 4.15 ppm due to the methylene moiety of the axial pyridylmethyl arm in  $[\text{Rh}^{\text{III}}(\text{L}_1\text{-H5})(\text{Cl})_2]$  decreased to about 50% of the original value for the singlet peak at 5.33 ppm observed for  $[\text{Rh}^{\text{III}}(\text{Cl})_2(\text{L}_1\text{-H6})]^+$  ([Figure 2](#)). These results indicate that deprotonation of  $[\text{Rh}^{\text{III}}(\text{Cl})_2(\text{L}_1\text{-H6})]^+$  occurs at the axial

pyridylmethyl group rather than at the equatorial pyridylmethyl groups.

To clarify the reason for the selectivity of the deprotonation at the axial methylene moiety, we evaluated the thermodynamic stability of  $[\text{Rh}^{\text{III}}(\text{L}_1\text{-H5})(\text{Cl})_2]$  (deprotonation from the methylene moiety of the axial pyridylmethyl arm) and  $[\text{Rh}^{\text{III}}(\text{L}_1\text{-HSeq})(\text{Cl})_2]$  (deprotonation from the methylene moiety of one of the equatorial pyridylmethyl arms), using density functional theory (DFT) calculations. As a result,  $[\text{Rh}^{\text{III}}(\text{L}_1\text{-H5})(\text{Cl})_2]$  was indicated to be more stable than  $[\text{Rh}^{\text{III}}(\text{L}_1\text{-HSeq})(\text{Cl})_2]$  by 9.8 kcal/mol. This difference should be derived from the conformational distortion of  $[\text{Rh}^{\text{III}}(\text{L}_1\text{-HSeq})(\text{Cl})_2]$  ([Figure S3](#)): The distortion of  $[\text{Rh}^{\text{III}}(\text{L}_1\text{-HSeq})(\text{Cl})_2]$  would be derived from the rotation around an N–Rh axis because of the sp<sup>2</sup> character of the deprotonated equatorial methylene carbon.

The structure of  $[\text{Rh}^{\text{III}}(\text{L}_1\text{-H5})(\text{Cl})_2]$  was further confirmed by X-ray crystallography ([Figure 3](#)).<sup>14</sup> The bond length of C1–

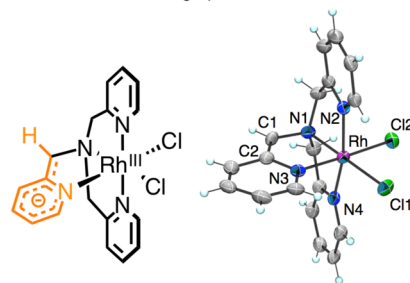
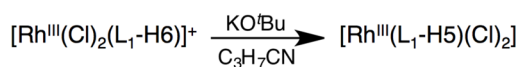


**Figure 3.** Schematic description of  $[\text{Rh}^{\text{III}}(\text{L}_1\text{-H5})(\text{Cl})_2]$  and an ORTEP drawing of the crystal structure.

C2 in  $[\text{Rh}^{\text{III}}(\text{L}_1\text{-H5})(\text{Cl})_2]$  (1.364(8) Å) is much shorter than that of  $[\text{Rh}^{\text{III}}(\text{Cl})_2(\text{L}_1\text{-H6})]^+$  (1.480(9) Å),<sup>12a</sup> as described in [Table S3](#) and [Figure S4](#). Judging from the structural change, a difference of bond lengths was mainly observed on the axial pyridine moiety in comparison with those of equatorial pyridine moieties even in the crystal. This result is consistent with those obtained from the spectroscopic measurements. The structure of  $[\text{Rh}^{\text{III}}(\text{L}_1\text{-H5})(\text{Cl})_2]$  also indicates that the dearomatized resonance structures of **B–D** ([Scheme 1](#)) of the axial pyridylmethyl moiety should be dominant in the actual structure of  $[\text{Rh}^{\text{III}}(\text{L}_1\text{-H5})(\text{Cl})_2]$  compared to the aromatic structure of **A** ([Scheme 1](#)). Also, the coordination of the pyridine N atom to a highly Lewis acidic Rh(III) center should stabilize the dearomatized resonance structure **D** ([Scheme 1](#)) of  $[\text{Rh}^{\text{III}}(\text{L}_1\text{-H5})(\text{Cl})_2]$  by trapping the negative charge on the N atom.

When we titrated  $[\text{Rh}^{\text{III}}(\text{Cl})_2(\text{L}_1\text{-H6})]^+$  with KO<sup>t</sup>Bu by using UV–vis spectroscopy in CH<sub>3</sub>CN at 294 K, 1 equiv of KO<sup>t</sup>Bu was consumed to complete the spectral change, which should be derived from the deprotonation of  $[\text{Rh}^{\text{III}}(\text{Cl})_2(\text{L}_1\text{-H6})]^+$  ([Figure 4a](#)). This result indicates that the further deprotonation of  $[\text{Rh}^{\text{III}}(\text{L}_1\text{-H5})(\text{Cl})_2]$  is negligible. Upon addition of 1,8-diazabicyclo[5.4.0]undec-7-ene (DBU) as a weaker base ( $\text{pK}_a = 24.3$  in CH<sub>3</sub>CN)<sup>15</sup> than KO<sup>t</sup>Bu, saturation behavior was observed in a titration plot ([Figure 4b](#)). The  $\text{pK}_a$  value of the axial methylene proton of  $[\text{Rh}^{\text{III}}(\text{Cl})_2(\text{L}_1\text{-H6})]^+$  was thus determined to be 27.3 in CH<sub>3</sub>CN at 294 K, according to the equation of the acid–base equilibrium ([Supporting Information Experimental Section](#)). Similarly, the  $\text{pK}_a$  value of  $[\text{Rh}^{\text{III}}(\text{Cl})_2(\text{L}_1\text{-H6})]^+$  in

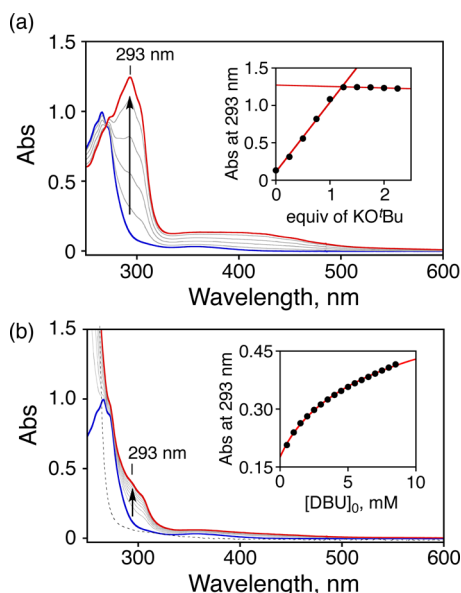


**Figure 4.** UV-vis spectra observed in titration of  $[\text{Rh}^{\text{III}}(\text{Cl})_2(\text{L}_1\text{-H}_6)]^+$  (0.10 mM) with (a)  $\text{KO}^t\text{Bu}$  or (b) DBU in  $\text{CH}_3\text{CN}$  at 294 K under Ar. Inset: Plots of Abs at 293 nm vs initial concentration of bases. A dotted line denotes the UV-vis spectrum of DBU (15 mM) in  $\text{CH}_3\text{CN}$ .

DMSO was also determined to be 16.1 by  $^1\text{H}$  NMR titration with potassium acetylacetonate ( $\text{pK}_a = 15.1$  in DMSO; **Figure S5**).<sup>16</sup> This  $\text{pK}_a$  value in DMSO was significantly smaller than that of 2-benzylpyridine as a reference compound without a Rh(III) ion ( $\text{pK}_a = 28.8$  in DMSO).<sup>16</sup> The large decrease of the  $\text{pK}_a$  value is derived from the stabilization of  $[\text{Rh}^{\text{III}}(\text{L}_1\text{-H}_5)(\text{Cl})_2]$  by coordination of deprotonated axial pyridine to a highly Lewis acidic Rh(III) center as evidenced by the analysis of the crystal structure shown in **Figure 3**.

If the localized negative charge of the dearomatized resonance structure **B** or **C** depicted in **Scheme 1** would be further stabilized by electron-withdrawing substituents introduced to the corresponding positions, then the deprotonated complex should be more stabilized. According to this hypothesis, COOMe groups as electron-withdrawing substituents were introduced to the 5-positions of all pyridyl groups of TPA as described in **Figure 1b**. A spectral change was detected for the  $^1\text{H}$  NMR spectrum of  $[\text{Rh}^{\text{III}}(\text{Cl})_2(\text{L}_2\text{-H}_6)]^+$  similar to that observed for  $[\text{Rh}^{\text{III}}(\text{Cl})_2(\text{L}_1\text{-H}_6)]^+$ , as depicted in **Figure S6**. This result indicates that one methylene proton of the axial pyridylmethyl arm in  $[\text{Rh}^{\text{III}}(\text{Cl})_2(\text{L}_2\text{-H}_6)]^+$  is removed to afford  $[\text{Rh}^{\text{III}}(\text{Cl})_2(\text{L}_2\text{-H}_5)]^+$ . The  $\text{pK}_a$  value of  $[\text{Rh}^{\text{III}}(\text{Cl})_2(\text{L}_2\text{-H}_6)]^+$  was determined to be 20.9 in  $\text{CH}_3\text{CN}$  at 296 K by UV-vis titration with triethylamine ( $\text{pK}_a = 18.8$  in  $\text{CH}_3\text{CN}$ ),<sup>15</sup> as shown in **Figure S7**. The lower  $\text{pK}_a$  value indicates that stabilization of the deprotonated complex is made through delocalization of the negative charge at the 5-position (dearomatized structure **B** in **Scheme 1**) into the methoxycarbonyl group. On the basis of the  $\text{pK}_a$  values of  $[\text{Rh}^{\text{III}}(\text{Cl})_2(\text{L}_1\text{-H}_6)]^+$  (27.3) and  $[\text{Rh}^{\text{III}}(\text{Cl})_2(\text{L}_2\text{-H}_6)]^+$  (20.9) in  $\text{CH}_3\text{CN}$ , we conclude that the deprotonated species derived from the latter is more stable by  $8.7 \text{ kcal mol}^{-1}$  ( $\Delta\Delta G^\circ$ ) than that derived from the former.

To develop reactivity of the Rh(III) complex having the deprotonated TPA ligand, we examined a reaction of the deprotonated Rh(III)-TPA complex with methyl iodide (MeI). Upon addition of MeI into the DMF solution of  $[\text{Rh}^{\text{III}}(\text{L}_1\text{-H}_5)(\text{Cl})_2]$ , methylation of  $[\text{Rh}^{\text{III}}(\text{L}_1\text{-H}_5)(\text{Cl})_2]$  occurred at 298

K. The structure of the isolated methylated product ( $[\text{Rh}^{\text{III}}(\text{Cl})_2(\text{L}_1\text{-H}_5\text{Me})]^+$  ( $\text{L}_1\text{-H}_5\text{Me}$  = methylated TPA) was determined by X-ray crystallography to reveal that the methylation occurred at the deprotonated axial methylene moiety (**Figure 5**). Because the methylation induces the chirality

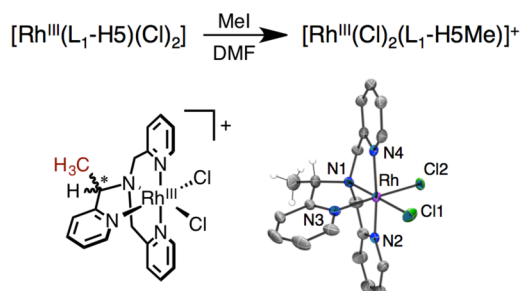


**Figure 5.** Methylation of  $[\text{Rh}^{\text{III}}(\text{L}_1\text{-H}_5)(\text{Cl})_2]$  and an ORTEP drawing of  $[\text{Rh}^{\text{III}}(\text{Cl})_2(\text{L}_1\text{-H}_5\text{Me})]^+$ .

at the methylene carbon, in the monoclinic crystal both enantiomers (the *R* and *S* forms) existed as a racemic mixture. The  $^1\text{H}$  NMR spectrum of  $[\text{Rh}^{\text{III}}(\text{Cl})_2(\text{L}_1\text{-H}_5\text{Me})]^+$  showed doublets due to the methyl group and the methylene proton of the reacted axial pyridylmethyl arm with the same coupling constant (6.8 Hz), together with two AX doublets (15.3 and 16.5 Hz) assigned to the equatorial methylene protons (**Figure S8**). These results indicate that the methylation of  $[\text{Rh}^{\text{III}}(\text{L}_1\text{-H}_5)(\text{Cl})_2]$  only occurs at the axial methylene position, although the negative charge should delocalize on the pyridine moiety as well.<sup>17</sup> The site selectivity of the methylation reaction mainly depends on the stability of the methylated product rather than the population of the negative charge because the methylation at the 3- or 5-position of the axial pyridine ring produces an unstable dearomatized product. The selective methylation of the axial methylene moiety is expected to embark a new method to provide a chiral TPA derivative by using a chiral reagent toward the development of TPA-based chiral catalysts for asymmetric transformation.

Redox properties of the deprotonated Rh(III)-TPA complexes were examined by cyclic voltammogram (CV) measurements in  $\text{CH}_3\text{CN}$ . The CV trace of  $[\text{Rh}^{\text{III}}(\text{L}_1\text{-H}_5)(\text{Cl})_2]$  exhibited only one irreversible anodic wave at 0.08 V vs SCE even at 233 K under Ar (**Figure S10**). In sharp contrast, a quasi-reversible redox wave was observed for  $[\text{Rh}^{\text{III}}(\text{L}_2\text{-H}_5)(\text{Cl})_2]$  with a peak separation ( $\Delta E_p = 75 \text{ mV}$ ; **Figure 6a**).<sup>18</sup> The one-electron

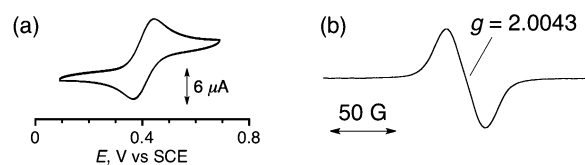


**Figure 6.** (a) CV of  $[\text{Rh}^{\text{III}}(\text{L}_2\text{-H}_5)(\text{Cl})_2]$  in  $\text{CH}_3\text{CN}$  at 233 K. (b) ESR spectrum of  $[\text{Rh}^{\text{III}}(\text{Cl})_2(\text{L}_2\text{-H}_5^\bullet)]^+$  measured at 100 K after the reaction of  $[\text{Rh}^{\text{III}}(\text{L}_2\text{-H}_5)(\text{Cl})_2]$  with  $[\text{Ru}^{\text{III}}(\text{bpy})_3]^{3+}$ .

oxidation potential ( $E_{1/2}$ ) of  $[\text{Rh}^{\text{III}}(\text{L}_2\text{-H}_5)(\text{Cl})_2]$  was determined to be 0.40 V vs SCE in  $\text{CH}_3\text{CN}$  at 233 K. The reversibility was drastically improved by the introduction of the electron-withdrawing COOMe groups to the 5-positions of pyridine rings to lower the SOMO level because the SOMO of one-electron oxidized  $[\text{Rh}^{\text{III}}(\text{L}_2\text{-H}_5)(\text{Cl})_2]$  ( $[\text{Rh}^{\text{III}}(\text{Cl})_2(\text{L}_2\text{-H}_5^\bullet)]^+$ ) was indicated to delocalize over the axial methylene moiety and the 3-



and 5-positions of the pyridine ring by DFT calculations (Figure S12). This reversibility allows us to elucidate the oxidation reaction as discussed below. To confirm that the oxidation of  $[\text{Rh}^{\text{III}}(\text{L}_2\text{-HS})(\text{Cl})_2]$  occurs at the metal center or the deprotonated TPA ligand, ESR measurements were performed on the solution of  $[\text{Rh}^{\text{III}}(\text{L}_2\text{-HS})(\text{Cl})_2]$  with addition of 1 equiv of one-electron oxidant such as  $[\text{Ru}^{\text{III}}(\text{bpy})_3]^{3+}$  (bpy = 2,2'-bipyridyl) at 100 K. As a result, a featureless ESR signal was observed at  $g = 2.0043$  (Figure 6b). Judging from the  $g$  value, the one-electron oxidation of  $[\text{Rh}^{\text{III}}(\text{L}_2\text{-HS})(\text{Cl})_2]$  takes place on the ligand to form a Rh(III) complex with a carbon-centered ligand radical ( $[\text{Rh}^{\text{III}}(\text{Cl})_2(\text{L}_2\text{-HS}^\bullet)]^+$ ) rather than at the Rh(III) center, in the light of the  $g$  value reported for  $[\text{Rh}^{\text{IV}}(\text{Cl})_6]^{2-}$  ( $g = 2.08$ ).<sup>19</sup> The carbon-centered radical was further confirmed by a reaction with a nitroxyl radical (2,2,6,6-tetramethylpiperidine 1-oxyl = TEMPO) in  $\text{CH}_3\text{CN}$  at 233 K; the spin adduct,  $[\text{Rh}^{\text{III}}(\text{Cl})_2(\text{L}_2\text{-HS-TEMPO})]^+$ , was characterized by ESI-MS and  $^1\text{H}$  NMR measurements (Figure S13).<sup>20,21</sup> Thus, this is the first observation of redox-noninnocent behavior of a metal-bound TPA ligand after deprotonation of a methylene proton of the ligand.

We have successfully demonstrated selective and reversible deprotonation of the methylene moiety of the axially coordinated pyridylmethyl arm of TPA ligands and the reactivity of the deprotonated TPA ligands in the Rh(III) coordination sphere. The deprotonation is governed by the stabilization of the dearomatized resonance structures (Scheme 1). For this reason, the coordination of a Lewis acidic metal ion and the introduction of electron-withdrawing groups to the position where the negative charge can be delivered in the resonance structures are effective. The deprotonation of the TPA ligand allows us to encounter unprecedented redox-noninnocent characteristics of the versatile tetradentate ligands involving a carbon-centered radical of metal-bound TPA. The results described in this paper will provide a basis for the development of new functionality of transition-metal-TPA complexes.

## ■ ASSOCIATED CONTENT

### Supporting Information

The Supporting Information is available free of charge on the ACS Publications website at DOI: 10.1021/jacs.5b06237.

Figures S1–S13 and Tables S1–S3. (PDF)

Crystallographic data for  $[\text{Rh}^{\text{III}}(\text{Cl})_2(\text{L}_2\text{-H6})]^+$ ,  $[\text{Rh}^{\text{III}}(\text{L}_1\text{-HS})(\text{Cl})_2]$ , and  $[\text{Rh}^{\text{III}}(\text{Cl})_2(\text{L}_1\text{-HSMe})]^+$  in the CIF format. (ZIP)

## ■ AUTHOR INFORMATION

### Corresponding Author

\*[kojima@chem.tsukuba.ac.jp](mailto:kojima@chem.tsukuba.ac.jp)

### Notes

The authors declare no competing financial interest.

## ■ ACKNOWLEDGMENTS

This work was partially supported by Grants-in-Aid (nos. 24245011 and 15H00915) from the Japan Society of Promotion of Science (JSPS, MEXT) of Japan, and the Cooperative Research Program of Network Joint Research Center for Materials and Devices. We thank Dr. Motoo Shiro (Rigaku Corp., Japan) for his kind help in X-ray analysis and Prof. Shigeru Yamago (Kyoto University) for his helpful suggestion on the radical trapping.

## ■ REFERENCES

- (a) Grützmacher, H. *Angew. Chem., Int. Ed.* **2008**, *47*, 1814–1818.
- (b) Gunanathan, C.; Milstein, D. *Acc. Chem. Res.* **2011**, *44*, 588–602.
- (c) Gunanathan, C.; Milstein, D. *Chem. Rev.* **2014**, *114*, 12024–12087.
- (2) Gunanathan, C.; Ben-David, Y.; Milstein, D. *Science* **2007**, *317*, 790–792.
- (3) (a) Ben-Ari, E.; Leitun, G.; Shimon, L. J. W.; Milstein, D. *J. Am. Chem. Soc.* **2006**, *128*, 15390–15391. (b) Zhang, J.; Leitun, G.; Ben-David, Y.; Milstein, D. *Angew. Chem., Int. Ed.* **2006**, *45*, 1113–1115.
- (4) (a) Lu, C. C.; Bill, E.; Weyhermüller, T.; Bothe, E.; Wieghardt, K. *J. Am. Chem. Soc.* **2008**, *130*, 3181–3197. (b) Shaffer, D. W.; Ryken, S. A.; Zarkesh, R. A.; Heyduk, A. F. *Inorg. Chem.* **2011**, *50*, 13–21.
- (5) (a) Büttner, T.; Geier, J.; Frison, G.; Harmer, J.; Calle, C.; Schweiger, A.; Schönberg, H.; Grützmacher, H. *Science* **2005**, *307*, 235–238. (b) Donati, N.; Stein, D.; Büttner, T.; Schönberg, H.; Harmer, J.; Anadaram, S.; Grützmacher, H. *Eur. J. Inorg. Chem.* **2008**, *2008*, 4691–4703.
- (6) Tejel, C.; Ciriano, M. A.; del Río, M. P.; Hettterscheid, D. G. H.; Tschlis i Spithas, N.; Smits, J. M. M.; de Bruin, B. *Chem. - Eur. J.* **2008**, *14*, 10932–10936.
- (7) (a) Jazdzewski, B. A.; Tolman, W. B. *Coord. Chem. Rev.* **2000**, *200*–202, 633–685. (b) Shimazaki, Y.; Yajima, T.; Tani, F.; Karasawa, S.; Fukui, K.; Naruta, Y.; Yamauchi, O. *J. Am. Chem. Soc.* **2007**, *129*, 2559–2568. (c) Storr, T.; Verma, R.; Pratt, R. C.; Wasinger, E. C.; Shimazaki, Y.; Stack, T. D. P. *J. Am. Chem. Soc.* **2008**, *130*, 15448–15459. (d) Pratt, R. C.; Lyons, C. T.; Wasinger, E. C.; Stack, T. D. P. *J. Am. Chem. Soc.* **2012**, *134*, 7367–7377. (e) Lyons, C. T.; Stack, T. D. P. *Coord. Chem. Rev.* **2013**, *257*, 528–540.
- (8) Anderegg, G.; Wenk, F. *Helv. Chim. Acta* **1967**, *50*, 2330–2332.
- (9) (a) Jacobson, R. R.; Tyeklar, Z.; Farooq, A.; Karlin, K. D.; Liu, S.; Zubietta, J. J. *J. Am. Chem. Soc.* **1988**, *110*, 3690–3692. (b) Lim, M. H.; Rohde, J.; Stubna, A.; Bukowski, M. R.; Costas, M.; Ho, R. Y. N.; Münck, E.; Nam, W.; Que, L., Jr. *Proc. Natl. Acad. Sci. U. S. A.* **2003**, *100*, 3665–3670. (c) Hirai, Y.; Kojima, T.; Mizutani, Y.; Shiota, Y.; Yoshizawa, K.; Fukuzumi, S. *Angew. Chem., Int. Ed.* **2008**, *47*, 5772–5776.
- (10) (a) Que, L., Jr.; Ho, R. Y. N. *Chem. Rev.* **1996**, *96*, 2607–2624. (b) Mirica, L. M.; Ottenwaelder, X.; Stack, T. D. P. *Chem. Rev.* **2004**, *104*, 1013–1045. (c) de Bruin, B.; Budzelaar, P. H. M.; Gal, A. W. *Angew. Chem., Int. Ed.* **2004**, *43*, 4142–4157.
- (11) Investigation on deprotonation of other metal-TPA complexes is currently ongoing in our laboratory.
- (12) (a) Lonnon, D. G.; Craig, D. C.; Colbran, S. B. *Dalton Trans.* **2006**, 3785–3797. (b)  $\text{Ru}^{\text{II}}$  complexes of  $\text{L}_2\text{-H6}$  have been reported; see Yamaguchi, M.; Kousaka, H.; Izawa, S.; Ichii, Y.; Kumano, T.; Masui, D.; Yamagishi, T. *Inorg. Chem.* **2006**, *45*, 8342–8354.
- (13) A similar  $^1\text{H}$  NMR spectral change due to the deprotonation of  $[\text{Rh}^{\text{III}}(\text{Cl})_2(\text{L}_1\text{-H6})]^+$  was also observed in  $\text{CD}_3\text{CN}$ , although the line broadening of the signals assigned to the axial pyridylmethyl moiety occurred by fast proton exchange between water and the highly basic deprotonated complex.
- (14) One of three independent  $[\text{Rh}^{\text{III}}(\text{L}_1\text{-HS})(\text{Cl})_2]$  structures in the asymmetric unit was selected. The ORTEP drawing containing the other  $[\text{Rh}^{\text{III}}(\text{L}_1\text{-HS})(\text{Cl})_2]$  structures also revealed a deprotonated form because there are no counteranions in the asymmetric unit.
- (15) Kaljurand, I.; Kütt, A.; Sooväli, L.; Rodima, T.; Mäimets, V.; Leito, I.; Koppel, I. A. *J. Org. Chem.* **2005**, *70*, 1019–1028.
- (16) Bordwell, F. G. *Acc. Chem. Res.* **1988**, *21*, 456–463.
- (17) The HOMO of  $[\text{Rh}^{\text{III}}(\text{L}_1\text{-HS})(\text{Cl})_2]$  was shown to delocalize on the methylene carbon, the 3- and 5-positions, and the N atom of the axial pyridine ring by DFT calculations (Figure S9).
- (18) The lifetime of  $[\text{Rh}^{\text{III}}(\text{Cl})_2(\text{L}_2\text{-HS}^\bullet)]$  was estimated to be 8.3 s on the basis of CV measurements (Figure S12).
- (19) Ellison, I. J.; Gillard, R. D. *Polyhedron* **1996**, *15*, 339–348.
- (20) Beckwith, A. L. J.; Bowry, V. W.; Ingold, K. U. *J. Am. Chem. Soc.* **1992**, *114*, 4983–4992.
- (21)  $[\text{Rh}^{\text{III}}(\text{Cl})_2(\text{L}_2\text{-HS-TEMPO})]^+$ : ESI-MS,  $m/z = 792.00$ ;  $^1\text{H}$  NMR (270 MHz,  $\text{CD}_3\text{CN}$ ), 6.32 ppm (s, CH), 4.98 and 5.72 ppm (2 ABq, 16 Hz,  $\text{CH}_2$ ).